579454

Sandia National Laboratories

Operated for the United States Department of Energy
by National Technology and Engineering Solutions
of Sandia, LLC.

Albuquerque, New Mexico 87185-0101
Livermore, California 94551-0969

date: June 21st 2023

to: WIPP Records Center

from: Seth King, 08881
Clifford Hansen, 08924
Priya Hora, 08718

subject: Evaluation of radiolytic gas generation from adsorbed water and from CPR materials, Revision 1

1. Introduction

In the Performance Assessment (PA) for the 1996 Compliance Certification Application, gas generation from radiolysis of water and cellulose, plastic, and rubber (CPR) was screened out as part of the features, events, and processes (FEPs) analysis due to low consequence to the long-term WIPP performance. These processes continued to be screened out of the WIPP PA until the 2019 compliance recertification application (CRA-2019), when gas generation from alpha radiolysis of water from radionuclides in solution and in wetted-solid form was screened in (Day 2019). Radiolysis of CPR continued to be screened out of the PA (Day 2019).

During the review of the CRA-2019, in completeness comment CC3-GEOCHEM-20 (Peake 2020), the EPA has raised the question of alpha radiolysis of water adsorbed on non-wetted solids:

> *The radiolytic hydrogen gas generation rate calculated for WIPP PA includes two processes: brine radiolysis due to dissolved and colloidal radionuclides in brine, and brine radiolysis caused by wetted solid radionuclides (Day 2019). Implementation of these processes in WIPP PA requires the presence of brine in the repository. Hydrogen gas production due to radiolysis of water adsorbed on various surfaces has also been reported in the literature (e.g., Laverne and Tandon 2003, La Caër 2011, Veirs et al. 2012). These data indicate that hydrogen gas yields at the oxide surface can be higher than in bulk water, due to the efficient energy transfer that can occur at the interface. The likely rates of hydrogen gas production due to radiolysis of adsorbed water on waste material surfaces should be evaluated to justify omitting this process from the gas generation calculations used in WIPP PA.*

This work evaluates the screening arguments for gas generation from the alpha radiolysis of adsorbed water on non-wetted solid radionuclides and of cellulose, plastic, and rubber.

WIPP:4.2.1:PA:QA-L:521584
Information Only

2. Radiolysis of adsorbed water in the unsaturated repository

Background on brine radiolysis in WIPP PA

To understand the issue of modeling radiolysis of water adsorbed on non-wetted solids, it is important to understand how brine radiolysis is currently modeled in WIPP PA. A complete description of the brine radiolysis model is given in Day (2019). The number of moles of each radionuclide, $M(t)$ [mol], is a function of the radionuclide decay constant, λ [1/s], the initial inventory of radionuclides M_0 [mol], the elapsed time, t [s], and the decay of any parent products. A closed-form analytical solution of the Bateman (1910) equation is used to calculate the number of moles of each radionuclide through time. The decay constant, λ, is a function of the radionuclide half-life, $T_{1/2}$ [s], as:

$$\lambda = \left(\frac{\ln(2)}{T_{\frac{1}{2}}} \right) \tag{1}$$

The mass of radionuclides in solution (dissolved and sorbed onto suspended colloids), $M(t)_{sol,i}$ [mol], is a function of the volume of computational cell, V [m^3], the porosity of the cell, ϕ, the brine saturation of the cell, S_w, the radionuclide mobilization potential, S_{sol} [mol/m^3], and the mole fraction of the radionuclide mf_i:

$$M(t)_{sol,i} = V \times \phi(t) \times S_w(t) \times S_{sol,i} \times mf_i(t) \tag{2}$$

The mass of wetted solid radionuclides, $M(t)_{wet}$ [mol], is the total inventory less the inventory in solution, multiplied by the brine saturation:

$$M(t)_{wet,i} = \left(M(t)_i - M(t)_{sol,i}\right) \times S_w(t) \tag{3}$$

Finally, the hydrogen generation rate for radionuclide i, $R_{H2,i}$ [mol/sec], due to brine radiolysis from radionuclides in solution and wetted solid is defined as:

$$R_{H2,i} = \left(M(t)_{sol,i} + M(t)_{wet,i} \times P_{dep}\right)\left(\lambda_i \times E_{dis,i} \times G(H_2)_{avg}\right) \tag{4}$$

where:

P_{dep} = energy deposition probability for wetted solids (GDEPFAC)

$E_{dis,i}$ = disintegration energy of radionuclide [eV/decay], i (DECAYNRG)

$G(H_2)_{avg}$ = average "G" value for H_2 [H_2 molecule/eV] (GH2AVG)

For the discussion of adsorbed water radiolysis, it is important to note that the terms for the mass of radionuclide in solution, $M(t)_{sol,i}$, and the mass of wetted solid radionuclide, $M(t)_{wet,i}$, are proportional to the brine saturation; thus, when brine saturation goes to 0, the hydrogen generation rate will also go to 0.

The energy deposition probability, P_{dep}, represents the fraction of disintegration energy from radionuclides in a wetted solid waste particle that goes into brine radiolysis. Some of the energy is self-attenuated by the solid oxide particle as a function of the particle size. Radionuclide particles with diameters greater than 20 µm release less than half of their disintegration energy (Day 2019). Figure 1 shows the fractional energy released as a function of waste particle size (Day 2019, DOE 2012, Tandon 2000).

Information Only

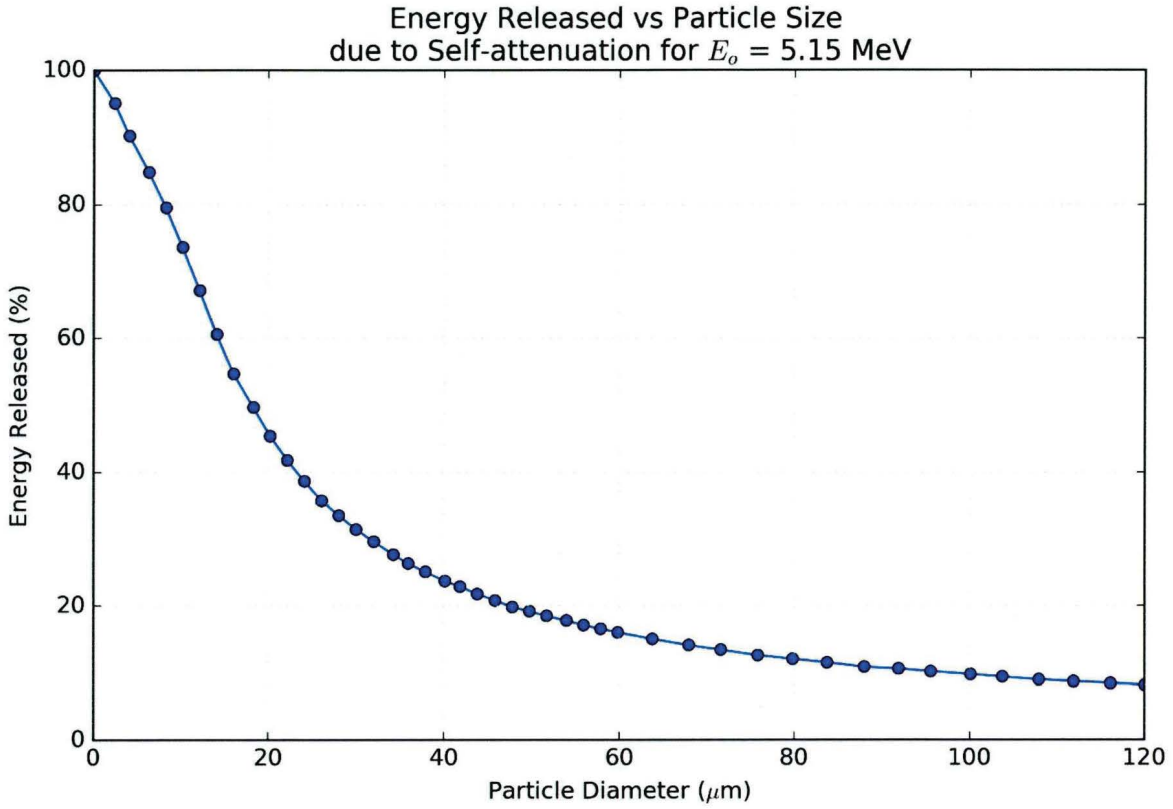

Figure 1 – Fractional Energy vs Waste Particle Diameter for PuO_2 (from Day 2019)

Five radionuclide isotopes are selected to represent the decay inventory for the brine radiolysis calculation: Pu238, Pu239, Pu240, Pu242, and Am241. As shown by Kicker (2019), these five isotopes represent over 95% of the decay energy of the WIPP inventory at any time during the regulatory life of the WIPP repository.

Brine radiolysis has two competing effects on releases. The generation of gas increases pressure in the repository, which increases the drive for direct brine releases (DBRs), spallings, and flow of contaminated brine away from the repository. However, the consumption of brine reduces the mobile brine availability for DBRs and for brine flow away from the repository. Brine radiolysis will have no impact on cuttings and cavings releases. The CCDF of mean total releases, on which WIPP long-term compliance is based, was dominated by cuttings and cavings at higher probabilities and DBRs at lower probabilities in the CRA-2019. The addition of brine radiolysis had no impact on mean total releases at high probabilities. At lower probabilities, the reduction in mobile brine availability had a slightly larger impact on DBRs than the increased pressure drive, leading to lower mean releases. The impact on the total mean release CCDF is shown in Figure 2.

Information Only

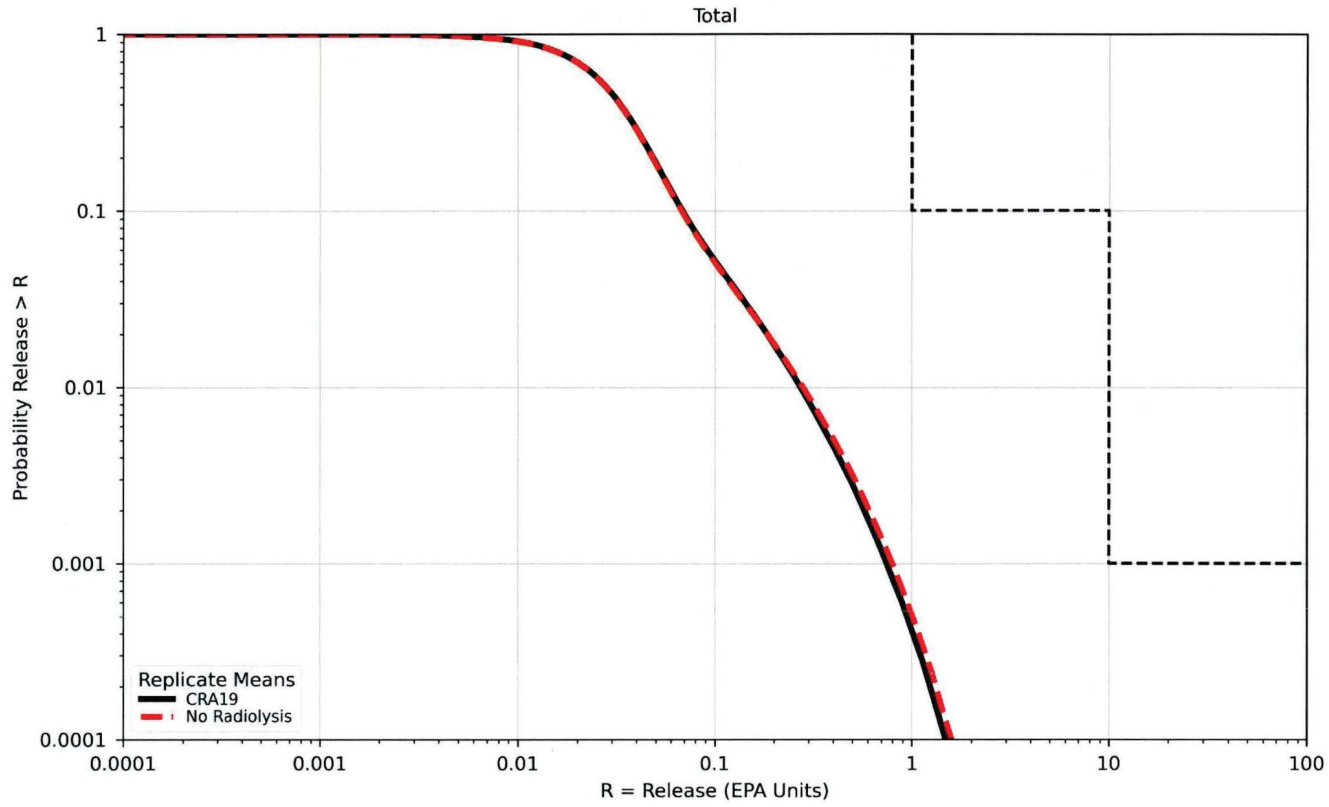

Figure 2 – Impact of brine radiolysis on mean total releases

Evaluation of literature

LaVerne and Tandon (2002 and 2003) studied H_2 production from the radiolysis of water adsorbed onto UO_2, CeO_2, and ZrO_2. These experiments used an external source of either gamma or alpha radiation. Due to the relatively low amount of gamma decay predominant in WIPP waste, radiolysis by gamma radiation would be minimal. Only the alpha radiation experimental results are relevant to WIPP PA.

In the LaVerne and Tandon (2002 and 2003) work, H_2 generation G-values larger than that of bulk water were observed, including physically impossible G-values over 40 molecules/100 eV. Sims et al. (2013) and Pastina and LaVerne (2021) evaluate this behavior and conclude that there is an energy transfer between the oxide surface and the adsorbed water. Sims et al. (2013) explains that, for the oxides studied by LaVerne and Tandon, the band gap energies fall within the range of 4.5 to 6 eV, which promote an energy transfer between the solid oxide and the adsorbed water which increases the H_2 yield. However, plutonium dioxide has a lower band gap energy of 1.8 eV, meaning its ability to promote hydrogen generation should be quite low. Due to the differences in atomic configuration and H_2 formation energetics seen in various reduced AnO_2 surfaces, results from studies focusing on mineral oxides other than Pu or Am may not be representative. Especially since, as pointed out above, Pu and Am isotopes contribute the majority of activity in the WIPP waste. That is, the experiments reported by LaVerne and Tandon containing UO_2, CeO_2, and ZrO_2 are not good analogs for radiolysis by the radionuclides that dominate the decay energy of the WIPP waste.

La Caër (2011) does not present new experimental work but provides an overview of water radiolysis with a focus on H_2 production. La Caër states that H_2 production is strongly modified at oxide surfaces. La Caër shows that there is an increased H_2 yield on the surface of oxides with the band gap between 4.5 to

Information Only

6 eV (Figure 1 of La Caër 2011). Much like the LaVerne and Tandon work above, these oxides are not representative of the Pu and Am that dominate the decay energy of WIPP waste, and this increased H_2 yield is not expected for adsorbed water radiolysis in the WIPP.

Veirs et al. (2012) study PuO_2 which is relevant to the WIPP inventory. The amount of water adsorbed onto the surface of PuO_2 is shown to be between 3 and 5 monolayers at the assumed WIPP relative humidity (RH) of 70 to 75% when brine is present. Veirs et al. (2012) study oxygen generation for radiolysis reactions and conclude that outside of 50 to 55% RH oxygen generation would not occur. Veirs et al. does not provide data on H_2 generation.

Sims et al. (2013) looked at radiolysis of water adsorbed on the surface of plutonium dioxide and saw G-values between 0.01 and 0.4 molecules/100 eV. All G-values observed by Sims et al. at less than 80% relative humidity and less than 6 monolayers of water are at least 1 order of magnitude less than the 1.4 mol/100 eV used in WIPP PA for brine radiolysis (Figure 3 and 4 of Sims et al. 2013).

Venault et al. (2019) looked at alpha radiolysis of water adsorbed on plutonium dioxide. Venault et al. used higher dose rates compared to Sims et al. but saw similar initial H_2 production. Venault et al. used a closed system and observed steady-state H_2 concentrations after several hundred hours, indicating an equilibrium between radiolytic reactions H_2 consumption reactions at higher H_2 partial pressures.

In conclusion, experiments conducted with Pu oxides by Sims et al (2013) are nearest to WIPP conditions; they report G-values lower than that used for radiolysis of brine. The results reported by Venault et al. (2019) appear to corroborate those of Sims et al. (2013).

Modeling radiolysis of adsorbed water

Water vapor pressures over brine solutions are dramatically lower than vapor pressures over pure water, resulting in lower relative humidity (RH) in the WIPP than in an environment with pure water. The gas phase in the WIPP when liquid brine is present is assumed to be at a relative humidity between 70% to 75%; Brush (2005) conducted a series of thermodynamic calculations for each of the brines expected in the WIPP showing an equilibrium relative humidity between 72.9% and 74.8%. This range agrees with studies of relative humidity over aqueous NaCl and MgCl solutions (Carr and Harris 1949; Greenspan 1977).

The depositional energy factor in the brine radiolysis model accounts for the amount of energy that is not self-absorbed by the solid oxide particle. When the solid particle is immersed in brine it is reasonable to assume in the model that all of the energy escaping the particle as going into radiolysis reactions. For brine immersed conditions, it would be expected that the energy transfer would decay with travel distance and all of the energy of an alpha particle would be transferred to radiolysis reactions within roughly 38 μm of travel (Morales et al. 2000). A single monolayer of water would have an expected thickness of 0.25 nm. With an expectation of 3 to 5 monolayers of water at 70 to 75% relative humidity (Veirs et al. 2012), the thickness of adsorbed water on the surface of the plutonium oxide would be orders of magnitude less than the travel distance of the alpha particle where energy is deposited into radiolysis reactions. Therefore, it would be expected that adsorbed water radiolysis reactions would generate less gas than immersed brine radiolysis reactions.

From Sims et al. (2013) the maximum G-value for adsorbed water at less than 80% relative humidity (<6 monolayers of water) is roughly 0.07 molecules/100 eV. Given the volume-averaged brine saturation in the waste area and the gas generated from brine radiolysis, an estimate of the gas that could be generated from adsorbed water radiolysis can be made with the ratio of G-values and ratio of gas saturation to brine saturation, that is:

Information Only

$$R_{ads,est} = R_{brine}\left(\frac{0.07\frac{mol}{100\ eV}}{1.4\frac{mol}{100\ eV}}\right)\left(\frac{1-\overline{S_w}}{\overline{S_w}}\right) \quad (5)$$

Figure 3 shows the mean gas generation from this estimate of adsorbed water radiolysis compared to the other gas generation mechanisms in CRA-2019. In the undisturbed scenario (S1-BF), adsorbed water radiolysis would generate roughly the same amount of gas as brine radiolysis, because mean brine saturation remains low. In all other scenarios, radiolysis of adsorbed water generates less gas than any other mechanism due to increased mean brine saturation.

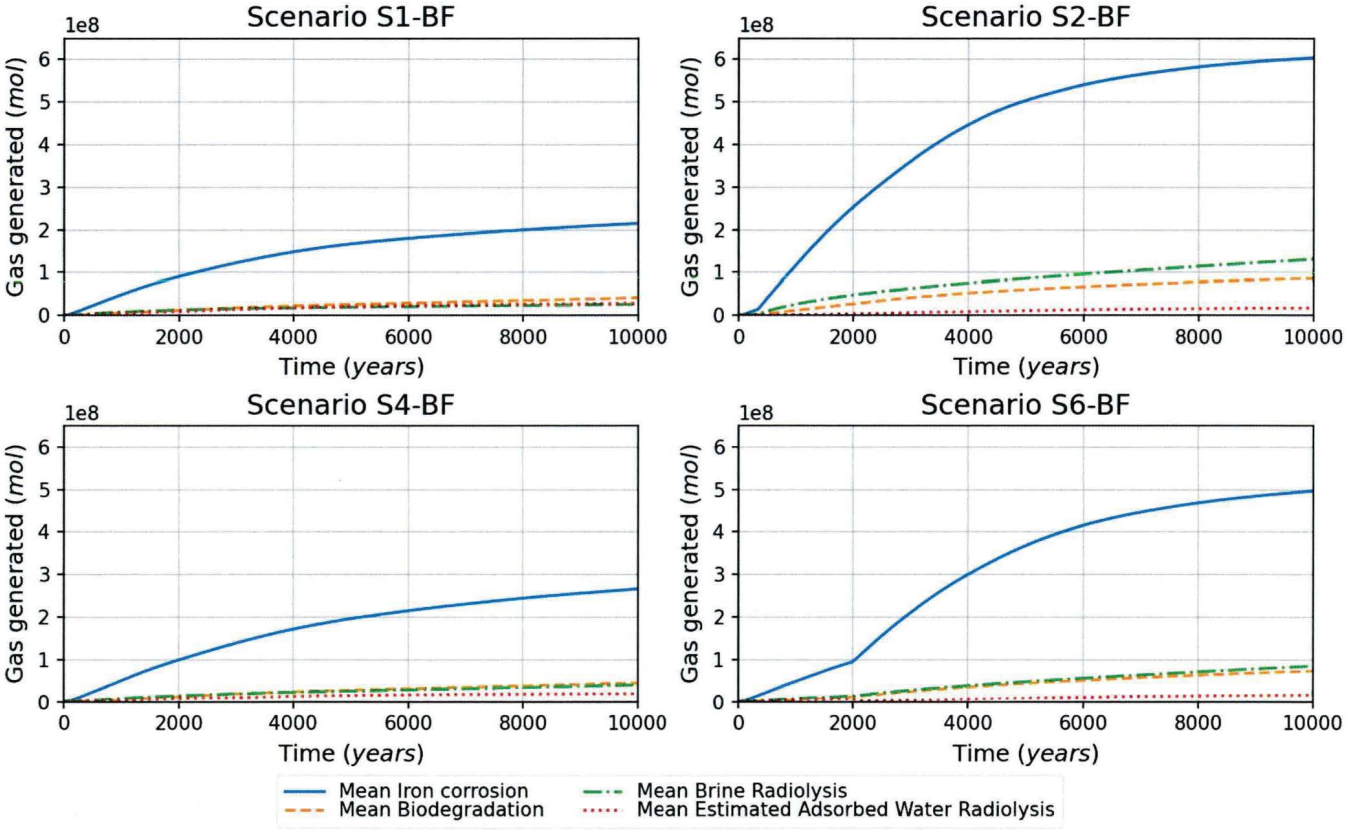

Figure 3 – Gas generation mechanisms from CRA-2019 plus an estimate of adsorbed water radiolysis

Eq. 5 does not account for the adsorbed water consumed by radiolysis. To maintain mass balance of water, an integrated model would be needed that removes adsorbed water consumed by radiolysis and that decreases relative humidity as brine saturation decreases. Physically it would also make sense that as brine saturation dropped very low (<1%) the relative humidity would drop and adsorbed water available to radiolysis would decrease. For these physical and numerical reasons, any adsorbed water radiolysis model should have a decreasing rate at low (<1%) brine saturations. For these reasons it is not appropriate to use Eq. 5 to represent radiolysis of adsorbed water in the WIPP PA models.

Gas generation models that consume brine introduce competing effects on releases – gas generation increases the pressure in the repository while also reducing the brine availability to carry mobile actinides. The addition of brine radiolysis to the PA model in CRA-2019 reduced mean total releases (Figure 2), as the reduced brine availability was a more important factor than was the increased pressure. Modeling adsorbed water radiolysis would likely further drive mean releases down. Because radiolysis of adsorbed water would add a minimal amount of gas generation as compared to other sources, including adsorbed

Information Only

water radiolysis would have a small and beneficial impact on releases and therefore can continue to be screened out of the PA.

Other conservativisms

Our analysis of the potential impact of radiolysis of adsorbed water involves several conservative approximations and assumptions. Containers are not considered an engineered barrier in the WIPP system, but these containers will isolate much of the waste from brine and humid air for many years after repository closure. Additionally, in the packaging of surplus plutonium, the Pu and adulterant are tightly compressed into a solid form. This means that the adulterant and other plutonium particles will very likely absorb alpha particles, self-attenuating that energy to a greater extent compared to small PuO_2 particles. Conservatism is introduced by treating the Pu as particles of small diameter.

Venault et al. (2012) showed a steady state of H_2 concentration as the H_2 partial pressure increased, indicating an equilibrium between radiolytic production of H_2 and H_2 consumption. Modeling the H_2 production from radiolysis without also accounting for any H_2 consuming reactions will tend to overestimate $H_2(g)$ in the repository. H_2 consumption is not accounted for in the model above.

Our analysis assumes equilibrium water conditions and does not consider the kinetics of water entering the vapor phase or adsorbing onto solid surfaces. It is possible that radiolysis could deplete the monolayers of adsorbed water faster than those monolayers of water are replenished, reducing the gas generation rate even when liquid brine is present.

For all of the above reasons, it is believed this is a conservative overestimation of adsorbed water radiolysis in the WIPP.

Information Only

3. Radiolysis of Cellulose, Plastic, and Rubber

Since the CCA, it has been recognized that only a small fraction of CPR material would be available to alpha particles for radiolytic reaction. The non-penetrating nature of alpha radiation would lead to depletion of hydrogen available to form gaseous molecules, a process, referred to as matrix depletion. This argument was restated in Day (2019) and in completeness comment response CC3-GEOCHEM-19 (Knerr 2020). It is believed that this argument remains valid, however the matrix depletion argument does rely on a structure to the CPR material which appears to conflict with the well-mixed batch-reactor modeling assumptions made for other WIPP PA chemistry models. There is no reason that a FEPs screening argument must incorporate the modeling simplifications and assumptions used to represent FEPs in the PA calculations. However, in this section we will show that in an assumed well-mixed system, CPR radiolysis can still be screened out of the PA calculation due to minimal impact.

If a well-mixed reactor is assumed, an alpha particle could interact with any of the waste material. The probability of an alpha particle interacting with CPR material could be estimated as the volume fraction of CPR material to other material. There is a total of 1.78E+07 kg of CPR in the Operational, Emplacement, Waste, and Packaging materials in the projected WIPP inventory (Van Soest 2018). Assuming densities of 1500 kg/m^3, 930 kg/m^3, and 1060 kg/m^3 for cellulose, plastic, and rubber respectively, there is an estimated volume of 1.65E+04 m^3 of CPR material in the WIPP inventory. The volume of the empty repository is 4.38E+05 m^3 (REFCCON:VREPOS), which is initially assumed to be 84% pore space giving 16% solid volume. With a total solid volume of 7.0E+04 m^3, and the estimated CPR material volume above, the CPR volume fraction is 24%. This estimate conservatively ignores the increase in volume metal corrosion would generally induce and the water present in the pore volume.

Given the average initial G-value of 1.25 molecules/100 eV from Zerwekh (1979), and the 4.71% volume fraction of CPR material above, an estimated mean CPR gas generation rate can be calculated as:

$$R_{cpr,est} = 0.24 * R_{brine} \left(\frac{1.25 \frac{mol}{100\ eV}}{1.4 \frac{mol}{100\ eV}} \right) \left(\frac{1}{\overline{S_w}} \right) \quad (6)$$

Information Only

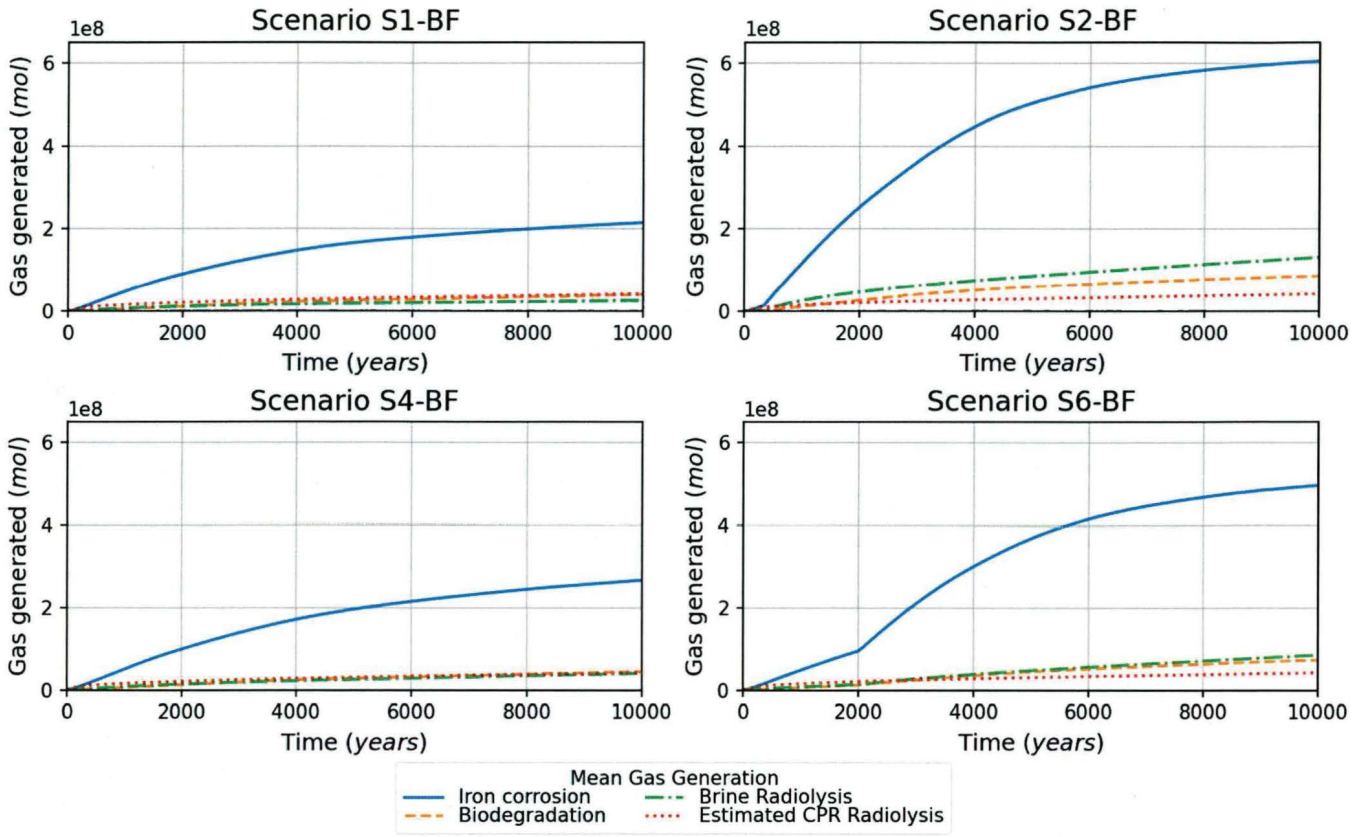

Figure 4 – Estimated CPR gas generation compared to other gas generation mechanisms

Figure 4 compares gas generation from this estimate of CPR radiolysis with the other gas generation mechanisms. Note that this estimate of the CPR gas generation does not account for the decay energy going into brine radiolysis, and therefore overstates the potential for CPR radiolysis. In this estimate, there is no functional dependence on repository conditions, such as brine saturation, so the same estimate of gas generated from CPR radiolysis would be obtained for all intrusion scenarios.

This estimate of the gas generation from CPR radiolysis using the batch reactor assumption is less than the estimated gas generation from CPR radiolysis using the matrix depletion argument presented in the response to CC3-GEOCHEM-19b (Knerr 2020). In the response to CC3-GEOCHEM-19b, a calculation is presented which shows that including CPR radiolysis would have minimal impact on the PA results. The same conclusion holds if the effect of CPR radiolysis is estimated assuming a well-mixed reactor. Therefore, CPR radiolysis can continue to be screened out of the PA calculation due to low impact.

Information Only

4. Conclusions

Radiolysis of water adsorbed on solid oxides in the WIPP repository has been investigated. Conditions in the WIPP repository favor limited monolayers of adsorbed water and the disintegration energy of radionuclides providing the majority of decay energy in the WIPP inventory is relatively low. Therefore, gas generation from radiolysis of adsorbed water would be small compared to gas generation from radiolysis of brine. Radiolysis of adsorbed water should continue to be screened out of the WIPP PA.

While it is believed the matrix depletion argument for CPR radiolysis is a sufficient basis for screening CPR radiolysis out of the WIPP PA, another screening argument is put forward that aligns with the simplifying well-mixed reactor assumption used for other WIPP PA models. With the well-mixed batch reactor assumption it is shown that the estimated gas generation from CPR radiolysis is less than the gas generation estimated using the matrix depletion argument. Because the higher level of gas generation from CPR radiolysis (from the matrix depletion argument) has already been shown to have minimal impact on the WIPP PA results, the new well-mixed batch reactor argument also supports screening CPR radiolysis out of the WIPP PA.

Revision History

This memo was revised for clarification based on comments made by the Carlsbad Field Office (CBFO). No substantial changes have been made to the results or conclusions.

Information Only

5. References

Bateman, H. 1910. The solution of a system of differential equations occurring in the theory of radioactive transformations. In Proc. Cambridge Philos. Soc. (Vol. 15, No. pt V, pp. 423-427).

Brush, L.H. 2005. Results of Calculations of Actinide Solubilities for the WIPP Performance Assessment Baseline Calculations. Analysis report, May 18, 2005. Carlsbad, NM. Sandia National Laboratories. ERMS 539800.

Carr, D.S., & Harris, B.L. 1949. Solutions for Maintaining Constant Relative Humidity. Industrial & Engineering Chemistry, 41, 2014-2015.

Day, B. 2019. Reassessment of Need and Parameter Justification for Modeling Gas Generation due to Radiolysis of Brine and Cellulose/Plastic/Rubber in WIPP for CRA-2019. Carlsbad, NM. Sandia National Laboratories. ERMS 570873.

Greenspan L. 1977. Humidity Fixed Points of Binary Saturated Aqueous Solutions. Journal of Research of the National Bureau of Standards. Section A, Physics and Chemistry, 81A(1), 89–96. https://doi.org/10.6028/jres.081A.011

Kicker, D. 2019. Radionuclide Inventory Screening Analysis for the 2019 Compliance Recertification Application Performance Assessment (CRA-2019 PA). Carlsbad, NM: Sandia National Laboratories. ERMS 571659.

Knerr, R. 2020. Response 7 to U.S. Environmental Protection Agency's 2019 Compliance Recertification Application Completeness Comments Letters dated May 6, 2020, June 12, 2020, July 17, 2020 and September 11, 2020 from Tom Peake to Mike Brown. U.S. Department of Energy, Carlsbad Field Office, Carlsbad, New Mexico. Letter to L.B. Veal, U.S. Environmental Protection Agency Radiation Protection Division, Washington, D.C. December 1, 2020.

LaVerne, J.A., and L. Tandon. 2002. H2 production in the radiolysis of water on CeO_2 and ZrO_2. Journal of Physical Chemistry B 106:380-386.

LaVerne, J.A., and L. Tandon. 2003. H2 production in the radiolysis of water on UO2 and other oxides. Journal of Physical Chemistry B 107:13623-13628.

Le Caër, S. 2011. Water radiolysis: influence of oxide surfaces on H2 production under ionizing radiation. Water 3:235-253.

Morales, L., R Behrens, J. Lyman, L. Tandon, J. Kennison, M. Paffett. 2000. The Scientific Basis for Plutonium Stabilization with Particular Emphasis on Gas Generation. Waste Management Conference. February 2000. Tucson, AZ.

Pastina, B., and J.A. LaVerne. 2021. An Alternative Conceptual Model for the Spent Nuclear Fuel-Water Interaction in Deep Geologic Disposal Conditions. Applied Sciences. 11, 8566.

Peake, T. 2020. Third Set of EPA Completeness Comments and Questions for Compliance Recertification Application 2019 (CRA-2019). U.S. Environmental Protection Agency, Center for Waste Management and Regulation, Washington, D.C. Letter to M. Brown, U.S. Department of Energy, Carlsbad Field Office, Carlsbad, New Mexico, June 12, 2020.

Sims, H. E., K. J. Webb, J. Brown, D. Morris, R. J. Taylor. 2013. Hydrogen yields from water on the surface of plutonium dioxide. Journal of Nuclear Materials. 437, 359-364.

Information Only

Tandon, L. 2000. Radiolysis of Salts and Long-Term Storage Issues for Both Pure and Impure PuO_2 Materials in Plutonium Storage Containers. Los Alamos, NM. Los Alamos National Laboratories. LA-13725-MS.

U.S. DOE. 2012. CH-TRU Payload Appendices, Rev. 3, December 2012. Carlsbad, NM.

Van Soest, G.D. 2018. Performance Assessment Inventory Report – 2018. Los Alamos National Laboratory Carlsbad Operations. Carlsbad, NM. LA-UR-18-31882.

Venault, L., A. Deroche, J. Gaillard, O. Lemaire, N. Budanova, J. Vermeulen, J. Maurin, N. Vigier, P. Moisy. Dihydrogen H2 steady state in α-radiolysis of water adsorbed on PuO2 surface. Radiation Physics and Chemistry. 162, 136-145.

Veirs, D.K., J.M. Berg and M.L. Crowder. 2012. The effect of plutonium dioxide water surface coverage on the generation of hydrogen and oxygen. MIS Program Report, Los Alamos National Laboratory, LA-UR-12-22377.

Zerwekh, A. 1979. Gas Generation from Radiolytic Attack of TRU-Contaminated Hydrogenous Waste. Los Alamos National Laboratory. Los Alamos, NM. LA-7674-MS.

Information Only